

## Atomic hydrogen treatment of nanodiamond powder studied with photoemission spectroscopy

M. Yeganeh,<sup>1</sup> P. R. Coxon,<sup>1</sup> A. C. Brieva,<sup>1</sup> V. R. Dhanak,<sup>2,3</sup> L. Šiller,<sup>1,\*</sup> and Yu. V. Butenko<sup>1,\*</sup><sup>1</sup>*School of Chemical Engineering and Advanced Materials, University of Newcastle upon Tyne, Newcastle upon Tyne, NE1 7RU, United Kingdom*<sup>2</sup>*CCLRC, Daresbury Laboratory, Warrington, Cheshire, WA4 4AD, United Kingdom*<sup>3</sup>*Physics Department, University of Liverpool, Liverpool L69 3BX, United Kingdom*

(Received 23 August 2006; published 5 April 2007)

The effect of atomic hydrogen treatment upon the surface of partially graphitized nanodiamonds has been studied by photoemission spectroscopy. The C1s core level peak and valence band spectra of a partially graphitized nanodiamond sample were compared with those following hydrogen treatment and following subsequent annealing. We have observed a difference in the binding energy of the  $sp^3$  component of the C1s peak and in the valence band which we believe can be assigned to either upward or downward band bending due to surface graphitization and hydrogenation of nanodiamonds, respectively. The data confirms that the graphitic layers which initially cover the nanodiamond particles can be removed through exposure to atomic hydrogen. This method could enable the preparation of hydrogen terminated and separate nanodiamond particles.

DOI: 10.1103/PhysRevB.75.155404

PACS number(s): 73.22.-f, 79.60.-i, 81.05.Uw, 81.65.-b

## I. INTRODUCTION

Diamond nanoparticles can be produced by the detonation of explosives with a negative oxygen balance in hermetic tanks.<sup>1-3</sup> Nanodiamonds (ND) produced by this method are usually called detonation ND and typically have a narrow size distribution: the majority of particle sizes lie within the range 2 to 20 nm with an average particle size of 4–5 nm.<sup>3,4</sup> Detonation ND is used in many different areas such as plating, metal matrix composites, magnetic recording systems, lubricating oils, polishing, adsorbents, and additives to polymers.<sup>3</sup>

During the detonation synthesis diamond nanoparticles form very tight aggregates with diameters ranging from hundreds of nanometers to even several micrometers.<sup>5-8</sup> At present, the nature of the bonding between the diamond particles within these aggregates is still unknown. It has been proposed that a cocrystallite phase between diamond crystallites is responsible for the hard aggregation, which is stronger than chemical bonding.<sup>5,7</sup> The problem of the deaggregation of detonation ND has attracted great attention.<sup>7-11</sup> The preparation of separate ND and specifically functionalized diamond nanoparticles can enable applications of ND in biology and electronics. For example, *in-vivo* imaging or fluorescent markers,<sup>12</sup> for attachment of proteins, DNA molecules or other biologically active moieties<sup>9,13,14</sup> and for developing new small ultraviolet light-emitting devices.<sup>15</sup>

A high resolution transmission electron microscopy study has shown that graphitization starts from the surface of individual ND crystallites.<sup>16</sup> Hence, one of the approaches for breaking the ND aggregates can be based on partial graphitization of ND followed by removal of graphite layers from the surface of ND crystallites and between their grain boundaries. Indeed, Xu and Xue<sup>7</sup> have developed a “graphitization-oxidation” method in which air oxidation is used to remove the surface graphite layers. This method resulted in a significant deaggregation of ND.<sup>7</sup>

The aim of this work is to employ atomic hydrogen treatment for etching the graphite layers formed on the ND sur-

face as a result of their partial graphitization. X-ray and ultraviolet photoelectron spectroscopy was used to monitor chemical composition of ND samples and their electronic structure during the experiments. Atomic hydrogen treatment should allow us not only to remove the graphite layers, but to also passivate the surface by saturating the dangling bonds of the surface carbon atoms with hydrogen-containing groups and thus prevent particles from the subsequent aggregation. Depending on the crystallographic index [(111), (110), or (100)] of a diamond surface and its structure a surface carbon atom can be terminated with one or two hydrogen atoms (C–H<sub>x</sub>, where  $x$  can be 1 or 2).<sup>17-19</sup> This is in contrast to the graphitization-oxidation method, where the formation of the ethereal group ( $\geq\text{C}-\text{O}-\text{C}\leq$ ) between particles can occur due to the presence of oxygen-containing groups on diamond surfaces after oxidation which hinders the complete deaggregation.<sup>7,9</sup> The preparation of hydrogen terminated ND crystals may open up new possibilities of ND applications in electronics and biology, since hydrogenated diamond crystals show a high  $p$ -type surface conductivity,<sup>20</sup> negative electron affinity,<sup>21-23</sup> and bio compatibility.<sup>24</sup>

It is worth noting that the electronic properties of nanodiamond are considered to be different from those for larger diamond crystals, and these have been studied by x-ray adsorption spectroscopy<sup>25,26</sup> and x-ray emission spectroscopy.<sup>27</sup> Previously no detailed photoemission studies of the electronic structure of nanodiamond have been carried out due to the strong charge buildup under photon irradiation. Our approach to nanodiamond treatment has allowed us to measure the valence band and C1s core level photoemission spectra of nanodiamond.

## II. EXPERIMENT

In this work a partially graphitized ND sample (referred to throughout this paper as the “initial ND”) was previously prepared from a sample of detonation ND by annealing in a vacuum of  $10^{-5}$  Torr at a temperature of 1420 K for 85 min

such as is described in Ref. 28. The detonation ND in this experiment was provided by the Lavrentiev Institute of Hydrodynamics (Siberian Branch of Russian Academy of Science, Novosibirsk, Russia) (Ref. 29) and was boiled in a concentrated mixture of  $\text{HClO}_4$  and  $\text{H}_2\text{SO}_4$  acids (1:1) then washed by hydrochloric acid and water in order to clean them from nondiamond carbon and metal impurities.<sup>4</sup>

High resolution transmission electron microscopy studies showed that the initial ND sample consists of diamond crystallites encapsulated within graphitelike shells.<sup>28,30</sup> The values of the diamond fraction in the sample is approximately 0.86.<sup>28</sup> Measurements of electrical resistivity of the sample<sup>30</sup> revealed that the process of ND graphitization at 1420 K results in the emergence of sample electrical conductivity.

The experiments were performed at station 4.1 at the Synchrotron Radiation Source, Daresbury Laboratory U.K. The annealed ND powder was ultrasonically dispersed in isopropanol and several drops of this suspension were deposited onto silicon wafer substrates. The initial ND sample was then dried in air and mounted onto the sample holder in which the sample was kept in good electrical contact with tantalum retaining clips. After this, it was transferred into an ultrahigh vacuum chamber with a base pressure in the range of  $10^{-10}$  mbar. However after the experiments involving treatments in hydrogen, the pressure was in the range of  $1-5 \times 10^{-9}$  mbar due to the presence of significant amount of residual hydrogen. Prior to the atomic hydrogen treatment the sample was heated at 1200 K for 10 min in order to remove oxygen-containing groups,<sup>31</sup> traces of solvent and water.

Atomic hydrogen was produced by the thermal cracking of hydrogen molecules into atomic hydrogen with a hot tungsten filament. The hydrogen pressure was  $\sim 10^{-5}$  mbar. The filament was located 7–10 mm away from the sample. Hydrogenation was conducted for 100 min, during which time the sample was heated by the light from the tungsten filament and no additional heating was applied. Measurements performed separately showed that radiative heating from the hot filament raised the sample temperature to about 500 K.

The valence band spectra were measured using a Scienta SES-200 analyzer with an incident photon energy of 55 eV. The binding energy scale of the spectra was calibrated using the Fermi edge position of a platinum foil that was in electrical contact with the sample. An overall energy resolution of 0.20 eV was determined from the width of the Fermi cut-off. The  $\text{C}1s$  core-level spectra were acquired with a CLAM2 hemispherical electron energy analyser and  $\text{Mg } K\alpha$  radiation (1253.6 eV) from a conventional x-ray source. Freshly cleaved graphite, HOPG (0001), was introduced into the chamber, and its  $\text{C}1s$  spectra were utilized for the calibration of the core-level binding energies. An overall energy resolution of 0.8 eV was determined from the Gaussian width of the  $\text{Pt}4f$  line from a platinum foil in good electrical contact with the sample.

The peaks of  $sp^2$  carbon were fitted using a Doniac-Šunjić line shape<sup>32</sup> convoluted with a Gaussian profile, while other peaks were fitted with the Lorentzian form convoluted with the same Gaussian. The Gaussian component accounts for the instrumental energy resolution together with the chemical disorder, while the Lorentzian accounts for the lifetime of the

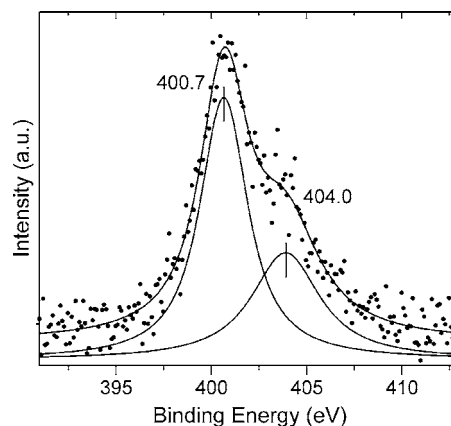


FIG. 1.  $\text{N}1s$  photoemission spectrum of the hydrogenated sample which reveals two peaks at binding energies of 400.7 and 404.0 eV. The dots represent experimental data and the solid lines are the fitted components from which the spectrum is composed. The background is subtracted by the Shirley method. The resulting fit is superimposed on the data. The spectrum was obtained using a photon energy of 1253.6 eV.

photoionization process.<sup>33</sup> The background of the photoelectron intensity was subtracted by the Shirley method.<sup>34</sup>

### III. RESULTS

Figure 1 shows the  $\text{N}1s$  photoemission spectrum of the initial ND sample together with the fitted curves. The spectrum was fitted with two peaks at binding energies of  $400.7 \pm 0.1$  and  $404.0 \pm 0.1$  eV. The ratio of atomic nitrogen to carbon was determined from their corresponding peak areas and taking into account sensitivity factors was found to be about 1–1.5%. The presence of nitrogen in the detonation ND may be accounted for by the presence of this element in the initial explosive mixture<sup>1–3</sup> and its possible incorporation into the diamond lattice during the detonation synthesis. It was found that nitrogen-containing species in carbon nitride films decay at temperatures higher than 1070 K.<sup>35,36</sup> In this work the initial ND sample was annealed at the higher temperature of 1420 K and therefore we believe that the nitrogen-containing species are absent from the graphitelike layers. Thus we suggest that the nitrogen signals observed in Fig. 1 are most likely due to nitrogen-containing species that remain in the diamond lattice. Full ND graphitization at 1900 K (Ref. 30) resulted in the complete loss of the nitrogen as evidenced by the absence of  $\text{N}1s$  peaks.

The  $\text{C}1s$  spectrum of the initial sample is presented in Fig. 2 and is fitted with four peaks at binding energies of  $284.7 \pm 0.1$ ,  $286.0 \pm 0.1$ ,  $286.6 \pm 0.1$ , and  $287.5 \pm 0.1$  eV with a full width at half maximum (FWHM) of  $1.5 \pm 0.1$  eV for all peaks. The first two peaks are related to  $sp^2$  and  $sp^3$  components, respectively. The positions of these peaks within experimental errors are in good agreement with the values reported previously for this sample in Ref. 37. The broadening of the  $\text{C}1s$  spectrum at higher binding energies is characterized by the peaks at  $286.6 \pm 0.1$  and  $287.5 \pm 0.1$  eV which together represent 36% of the total  $\text{C}1s$  peak area. These two peaks may be related to different oxygen-containing

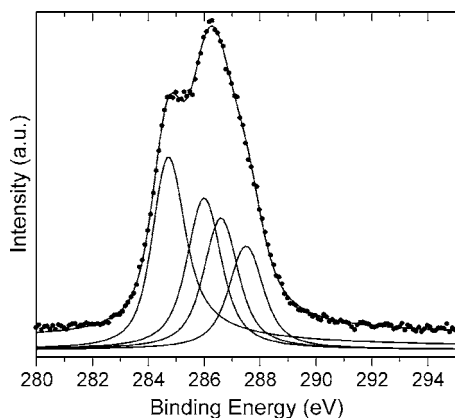


FIG. 2. C1s photoemission spectrum of ND annealed at 1420 K. The dots show the experimental data and the solid lines are the fitted components of which the spectrum was composed. The background is subtracted by the Shirley method. The resulting fit is superimposed on the data. The spectrum was obtained using a photon energy of 1253.6 eV.

groups.<sup>37</sup> However, analysis of the O1s photoemission spectrum of the initial ND (not presented here) has shown that the sample oxygen content is about 1%, since it had been outgassed in vacuum at 1200 K. Therefore we do not expect oxygen-containing groups to remain in such relatively large concentrations. The broadening could also be due to the contribution from carbon-nitride species<sup>38</sup> although the small concentration of nitrogen in the sample (1–1.5%) would not account for such a high proportion of carbon atoms (36%) with high binding energies of the C1s electrons. Therefore, the chemical shift alone cannot account for the high binding energy of these peaks.

Figure 3 illustrates the changes in the C1s photoemission spectrum of the ND sample following atomic hydrogen treatment and subsequent annealing at 1000 and 1200 K for 20 min. The C1s photoemission spectrum of the initial ND sample is presented in Fig. 3(a). The C1s photoemission spectrum of the sample after treatment by hydrogen [Fig. 3(b)] reveals a shift of the  $sp^3$  peak towards a higher binding energy ( $\sim 286.9$  eV) and the disappearance of the shoulder assigned to  $sp^2$  carbon. This result shows that surface graphitelike layers of partially graphitized ND particles have been etched away by the atomic hydrogen. This graphitelike carbon can be removed by the following reversible reaction:<sup>39</sup>



Further evidence for the removal of the graphitic layers by atomic hydrogen exposure is gained through an examination of sample charging effects upon photon irradiation (see below). Positive charging upon photon irradiation of the sample was observed to appear after its atomic hydrogen etching. This indicates that “bare” ND particles have a non-conductive nature. The charging of ND particles can account for the high binding energy of the  $sp^3$  peak centred approximately at 286.9 eV [Fig. 3(b)] compared to that observed for the initial ND sample at  $286.0 \pm 0.1$  eV [see Fig. 3(a)]. This latter value of binding energy was taken from the position of the  $sp^3$  component in the Fig. 2.

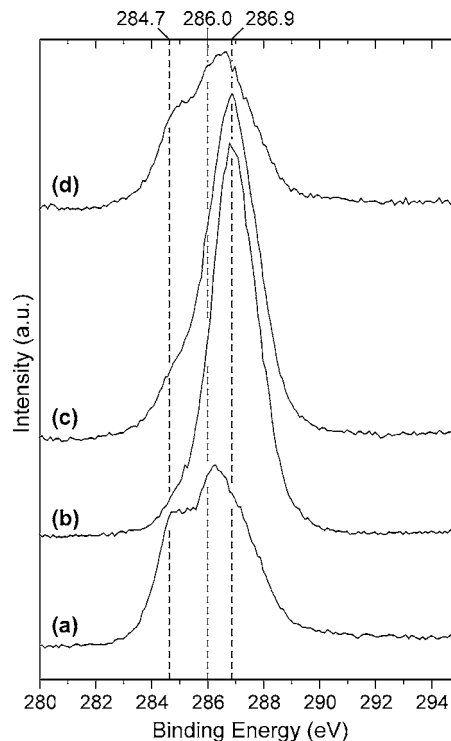


FIG. 3. C1s photoemission spectra of (a) the initial ND sample; (b) the same sample after atomic hydrogen treatment; (c) following additional annealing at 1000 K after hydrogenation; (d) following additional annealing at 1200 K after treatment described in (c). The annealing time was 20 min for both temperatures. Dashed lines are used to guide eyes. The binding energies of 284.7 and 286.0 eV were taken from the fitted components of Fig. 2. The spectra were obtained using a photon energy of 1253.6 eV.

In Fig. 3(c) we present the C1s photoemission spectra of the sample heated at 1000 K after hydrogenation. One can clearly observe the appearance of the small  $sp^2$  component at a binding energy of approximately 284.7 eV indicating the onset of the ND graphitization. Additional experiments confirmed that the sample does not experience charging under photon irradiation (see below), in contrast to the case after hydrogenation but before annealing. We observe a rather surprising result that upon nascent graphitization and the disappearance of the charging effect the  $sp^3$  peak remains at the same binding energy of  $\sim 286.9$  eV [Fig. 3(c)] as the hydrogenated nanodiamonds [Fig. 3(b)]. Possible reasons for this will be discussed in the next section.

Annealing at 1200 K causes further sample graphitization. The sample C1s photoemission spectrum presented in Fig. 3(d) is similar to the spectrum of the initial ND sample [Fig. 3(a)]. The spectrum was fitted with two peaks for  $sp^2$  and  $sp^3$  components with binding energies of  $284.7 \pm 0.1$  and  $286.0 \pm 0.1$  eV, respectively and two components with binding energies of  $286.6 \pm 0.1$  and  $287.5 \pm 0.1$  eV to account for the spectrum broadening at high binding energy. The FWHM of these peaks is  $1.5 \pm 0.1$  eV. The fitting curves are not presented in the figure.

In order to check the possible presence of sample positive charging under photon irradiation we performed several test experiments in which photoemission spectra were measured

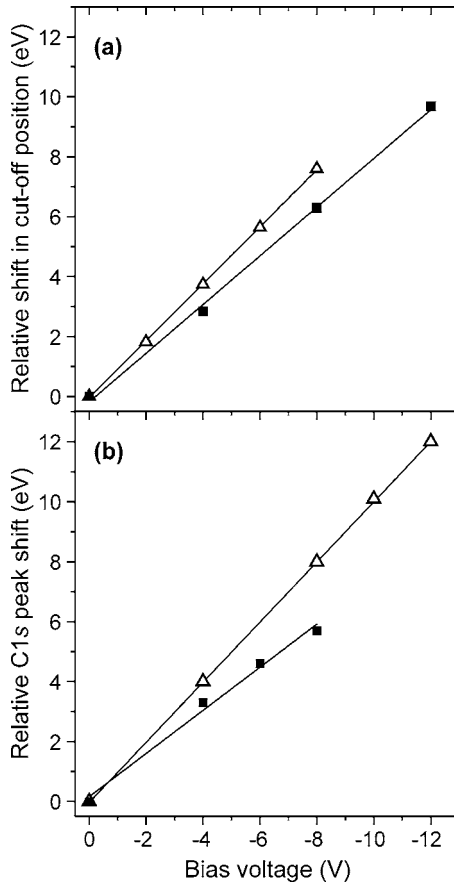


FIG. 4. (a)  $E_{\text{cut-off}}$  and (b) C1s peak position of the sample as a function of applied negative bias voltage after the sample was treated with atomic hydrogen (full squares) and after annealing at 1000 K (open triangles).

as a function of an applied negative bias voltage. This method has been previously described in Refs. 18 and 22. Figures 4(a) and 4(b) show the variation of the low-energy cut-off position,  $E_{\text{cut-off}}$ , of secondary electron emission and the C1s binding energy as a function of bias voltage applied to the sample holder, respectively. For the sample treated with atomic hydrogen (full squares), the observed shifts of the sample cut-off energy and C1s line are not proportional to the applied bias voltage (slope is  $0.81 \pm 0.01$ ) indicating a positive charge build-up at the sample surface under photon irradiation. Following heat treatment of the sample at 1000 K [open triangles in Figs. 4(a) and 4(b)] results in the vanishing of the charging effect since the shifts of the cut-off energy and C1s peak are proportional to the applied bias and a straight line with a unity slope is obtained. No charging effect was observed for the partially graphitized ND samples: initial ND sample and sample annealed at 1200 K after hydrogenation.

Figure 5 shows the evolution of the valence band following the sample treatments. The spectrum of the initial ND sample, Fig. 5(a), shows two prominent sharp peaks at  $3.2 \pm 0.2$  and  $7.8 \pm 0.2$  eV. The peak at 3.2 eV is attributed to  $\pi$  bonding in graphite,<sup>27,37,40,41</sup> the peak at 7.8 eV is related to  $\sigma$  bonding in graphite.<sup>27,37,40,41</sup> It should be noted that the spectrum does not contain the O2s peak, which for polycrys-

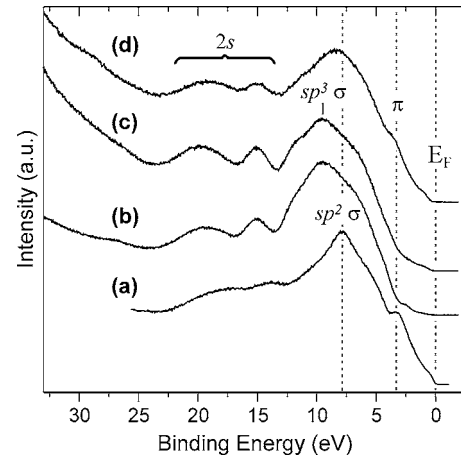


FIG. 5. Valence band spectra of (a) the initial ND sample annealed to 1420 K, (b) the same sample after atomic hydrogen treatment, (c) the additional annealing at 1000 K after hydrogenation, (d) additional annealing at 1200 K after treatment described in (c). Dashed lines are used to guide eyes.  $E_F$  is the Fermi energy level. The spectra were obtained using a photon energy of 55 eV.

talline diamond films treated by oxygen<sup>23</sup> and a diamond (100) crystal<sup>42</sup> is found at a binding energy of 23 eV. This confirms the absence of oxygen impurities, as the sample had been outgassed at 1200 K.

The spectrum of the hydrogenated sample in Fig. 5(b) contains three peaks at  $9.5 \pm 0.2$ ,  $15.1 \pm 0.2$ , and  $19.5 \pm 0.4$  eV. The peaks at 15.1 eV and 19.5 eV are attributed to C2s states.<sup>43</sup> The new pronounced peak at  $9.5 \pm 0.2$  eV is related to  $\sigma$  bonding in diamond.<sup>43</sup> In comparison to Fig. 5(a) we also observe the disappearance of the  $\pi$  peak at 3.2 eV which confirms that the graphiticlike layers have been successfully removed from the ND surface by the atomic hydrogen treatment. The significant drop in the density of states near the Fermi level ( $E_F$ ) is consistent with the observed poor sample electrical conductivity shown through the positive charge buildup under photon irradiation (see Fig. 4).

The valence band spectrum of the sample annealed after hydrogenation at 1000 K for 20 min [Fig. 5(c)] displays similar features as those in Fig. 5(b) which indicates a small progression in the graphitization process. However, some increase in the density of states near the Fermi level is observed which is consistent with appearance of electrical conductivity of the sample judged from the disappearance of the positive charging of the sample under photon irradiation (see Fig. 4). Figure 5(d) presents the valence band spectrum of the sample after annealing at 1200 K for 20 min. One can clearly see that further annealing at a higher temperature resulted in a more significant extent of the ND graphitization as evidenced by the reappearance of the  $\pi$  peak, the shift of the peak corresponding to  $\sigma$  bonds to lower binding energy and a further increase in the density of states near the Fermi level.

#### IV. DISCUSSION

The presence of nitrogen in pristine detonation ND was observed by Fourier transform infrared spectroscopy.<sup>44</sup> The

nitrogen impurities contribute to the broad bands at 1500–1000  $\text{cm}^{-1}$  in the infra red spectra of detonation ND, which denotes the presence of nitrogen atoms having three neighbor carbon atoms (tetrahedral bonding).<sup>35,44</sup> We observe nitrogen (Fig. 1) in ND partially graphitized at 1420 K. Due to the limited thermal stability of nitrogen-containing species in carbon materials<sup>35,36</sup> it is likely that nitrogen is embedded into the diamond lattice and is not present in the sample surface graphite layers. According to the XPS data (Fig. 1), there are at least two forms of nitrogen-containing species in the initial ND sample. The first line at a binding energy of  $400.7 \pm 0.1$  eV could belong to substitutional nitrogen atoms having three neighbor carbon atoms ( $-\text{N} <$ ).<sup>45</sup> Kusunoki *et al.*<sup>46</sup> noted that this binding energy is a little higher than the typical value of  $\sim 400$  eV for the  $-\text{N} <$  species, denoting that the nitrogen atoms could be slightly positively charged. The second peak at a binding energy of  $404.0 \pm 0.1$  eV is very difficult to assign (Fig. 1). Tillborg *et al.*<sup>47</sup> found that the  $\text{N}1s$  line for nitrogen physisorbed on graphite is centred at 403.9 eV, this value of binding energy is close to that observed in this work, therefore we suggest that the peak at binding energy of 404.0 eV may be related to trapped molecular nitrogen in the nanodiamond lattice.

The substitutional nitrogen in diamond forms a deep donor level with an energy 1.7 eV below the conduction band minimum,<sup>48,49</sup> therefore at room temperature nitrogen-doped diamond has a high electrical resistivity which explains the buildup of charge under photon irradiation during the experiments. One possible way to avoid this sample charging effect in photoemission measurements within nitrogen-doped diamonds is to heat the samples to above room temperature in order to thermally activate conduction. For example, Diederich *et al.*<sup>50</sup> kept a nitrogen-doped diamond substrate at a temperature of 400 °C while performing photoemission experiments. The authors of that work used a commercial diamond sample grown using high-pressure techniques. In contrast to nitrogen-doped high-pressure synthetic diamonds and detonation ND used in this work, nitrogen-doping of ultrananocrystalline diamond (UNCD) films synthesized by a chemical vapor deposition (CVD) technique increases the electrical conductivity of the UNCD substrates.<sup>51</sup> CVD synthesis produces UNCD films consisting of ND crystallites bonded together by grain boundaries involving a disordered mixture of  $sp^2$ ,  $sp^{2+x}$ ,  $sp^3$ , and dangling bond configurations.<sup>52</sup> Theoretical calculations have shown that nitrogen impurities in UNCD films are accumulated in the grain boundaries rather than in the bulk diamond.<sup>53</sup> Therefore, it was proposed that the formation of new electronic states in the diamond band gap associated with nitrogen impurities present in the grain boundaries is responsible for  $n$ -type high conductivity of nitrogen-doped UNCD.<sup>49,51,53</sup> This is in contrast to detonation ND where nitrogen atoms are most likely incorporated into the bulk.

We have observed that atomic hydrogen etches away surface graphite layers of partially graphitized diamond nanocrystallites. After this treatment remaining carbon atoms on diamond surfaces should be saturated by hydrogen atoms as it was observed for bigger diamond crystals.<sup>17–19</sup> According to temperature programmed desorption data<sup>31</sup> the hydrogen starts to desorb from ND surfaces at 1000 K. The decompo-

sition of hydrogen-containing groups and the simultaneous development of graphitization in our work [see appearance  $sp^2$  component in the spectrum presented in the Fig. 3(c)] agrees well with the results of theoretical works<sup>25,54–56</sup> which have demonstrated that hydrogen termination stabilizes ND surfaces and prevents their spontaneous graphitization.

The duration of the experiments with hydrogenated ND was almost 18 h (from the moment of the hydrogenation to annealing at 1000 K). During this time the sample remained stable and no graphitization was detected even after a 7 h exposure to vacuum ultraviolet radiation (55 eV). The stabilization of ND by hydrogen can be explained by considering the graphitization process itself. It has been shown that graphitization of ND crystallites begins at their surfaces.<sup>16</sup> This can be more readily understood by the fact that since the surface carbon atoms are bonded to fewer carbon atoms, they are much more mobile than those within the bulk material. Consequently, the presence of additional surface atoms (such as hydrogen) can make the surface carbon atoms of diamond behave more like those in the bulk material, and therefore can inhibit graphitization.

For ND hydrogen desorption begins at approximately 1000 K and finishes at approximately 1300 K.<sup>31</sup> As a result the heating at 1000 K for 20 min is likely to be insufficient to remove all surface hydrogen-containing groups. Indeed we observe the resemblance of the valence band spectra of the hydrogenated and heated at 1000 K samples [see Figs. 5(b) and 5(c)] and the same binding energy of the main  $\text{C}1s$  peak of these samples [see Figs. 3(b) and 3(c)]. Annealing at the higher temperature of 1200 K results in deeper decomposition of hydrogen-containing groups and more progress of ND graphitization which can be observed in resemblance of the  $\text{C}1s$  spectra of the initial ND sample [Fig. 3(a)] and the ND sample partially graphitized at 1200 K [Fig. 3(d)].

The first sign of ND graphitization is detected in the  $\text{C}1s$  photoemission spectrum of ND annealed at 1000 K [see Fig. 3(c)] and only annealing at 1200 K causes noticeable changes in both the  $\text{C}1s$  spectrum [see Fig. 3(d)] and the valence band spectrum [see Fig. 5(d)]. Such thermal stability is higher than that for diamondlike carbon (DLC) (Ref. 57) and is characteristic of diamond. For example, for DLC changes in the valence band spectra related to graphitization have been observed at temperatures as low as 350 °C.<sup>58</sup> This indicates that atomic hydrogen treatment of partially graphitized ND only etches away the graphitelike surface layers and leaves diamond structure of the remaining ND cores undamaged.

However, the structure of hydrogenated diamond nanocrystal surfaces is not clear. Low energy electron diffraction studies have demonstrated that for large diamond crystals hydrogen termination results in different surface reconstructions depending upon the type of a diamond surface.<sup>17–19</sup> The question of whether this situation is the same for diamond crystals of nanoscale dimensions, or if hydrogen termination will cause amorphization of ND surfaces for example, is still unknown. Surfaces of ND crystallites can display several facets (see HRTEM images of ND crystallites in Ref. 3) just as for surfaces of large diamond crystals. For diamond nanocrystallites theoretical studies<sup>55,56</sup> have shown that hydrogenation stabilized not only bulk but also surface dia-

mond structures and no transformations to amorphous  $sp^3$  carbon with C–H bonds on diamond surfaces were observed. Therefore we believe that hydrogenation does not cause amorphization of the diamond nanocrystallite surfaces and we expect that any induced surface reconstructions by hydrogenation would be similar to those for large diamond crystals.

Further evidence for the formation of hydrogen terminated ND crystallites is provided by consideration of the shift of 0.9 eV towards higher binding energy of  $sp^3$  C1s peak for the hydrogenated ND samples [the Figs. 3(b) and 3(c)] compared to that for the partially graphitized ND samples [Figs. 3(a) and 3(d)]. Smentkowski *et al.*<sup>18</sup> and Diederich *et al.*<sup>50</sup> provided a cogent explanation for the changes of the C1s binding energy upon deuteration (hydrogenation) and heat treatment of nitrogen- (boron-) doped diamond crystals. Partial surface graphitization of ND crystallites results in the formation of occupied and unoccupied  $\pi$  surface states. The unoccupied  $\pi$  states are filled by electrons from donor nitrogen atoms located in the bulk of remaining diamond cores.<sup>50</sup> This redistribution of electrons causes upwards band bending and the appearance of an electric field at the diamond–graphite interface, which influences the photoelectron kinetic energy and thus causes the C1s core level to shift to a lower binding energy.<sup>18,50</sup> On the other hand, when the atomic hydrogen removes the graphite layers and saturates the surface carbon atoms by hydrogen the  $\pi$  surface states should be removed. Vanishing of the surface states due to hydrogen termination causes downward band-bending, resulting in the C1s core level shift back to higher binding energies. In our experiments a nitrogen-doped ND sample was used and therefore the opposite behavior of its photoemission features depending upon surface treatments was observed compared to boron-doped diamond crystals.<sup>19,50</sup>

The broadening at high binding energy described by the peaks at  $286.6 \pm 0.1$  and  $287.5 \pm 0.1$  eV in the C1s spectra of the partially graphitized ND samples [Figs. 2, 3(a), and 3(d)] is possibly due to a different degree of band bending<sup>18,50</sup> for ND particles with different sizes and therefore possible different position of corresponding  $sp^3$  components in their C1s spectra.

The effect of band bending on the valence band spectrum of hydrogenated ND can be observed by its comparison with hydrogenated boron-doped diamond crystals.<sup>17,19,59,60</sup> Francz *et al.*<sup>60</sup> studied boron-doped natural diamond single crystals (type IIb). Figures 6(a) and 6(b) present valence band spectra of hydrogenated diamond crystals from their work. The spectra were obtained using a photon energy of 40.8 eV (He II). Valence band spectrum of hydrogenated and annealed ND at 1000 K in our work obtained at photon energy 55 eV is shown on Fig. 6(c). The spectrum of the hydrogenated and annealed ND at 1000 K is presented because this sample is not charged under photon radiation in contrast to the fully hydrogenated ND. However this sample can also be considered as a hydrogenated sample, since as it has been shown above that annealing the hydrogenated ND at 1000 K most likely results in only partial dehydrogenation of sample surfaces. This can be demonstrated by similarities in their valence band spectra [see and compare Figs. 5(b) and 5(c)]. For

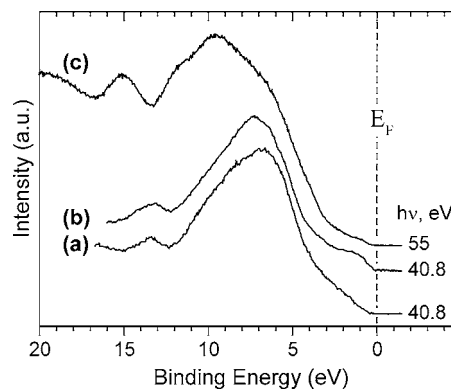


FIG. 6. Valence band spectra of (a) diamond (111) surface from Ref. 60; (b) diamond (100) surface from Ref. 60; (c) hydrogenated ND annealed at 1000 K [the same spectrum as in Fig. 5(c)]. Corresponding excitation energies are presented on the right side of the figure.

hydrogenated nitrogen-doped ND a shift of all valence band spectral features towards higher binding energies due to downward band bending is observed [Fig. 6(c)], which is in contrast to a shift to lower binding energies (upwards band bending) for hydrogenated boron-doped diamond crystals [Figs. 6(a) and 6(b)].

Nitrogen impurities present in detonation ND can influence not only the electronic structure of the sample, but also may affect the ND graphitization rate. Nitrogen substitutional atoms are defects in diamond lattice, and so it is reasonable to expect that they can facilitate the graphitization process. However, the concentration of nitrogen in detonation ND is only around 1–1.5%, therefore its influence on the ND graphitization should be negligible.

Annealing ND can activate diffusion of nitrogen-containing defects in ND from the bulk towards the crystallite surfaces. The rate of nitrogen diffusion can be larger than the rate of ND graphitization and therefore during ND annealing nitrogen can be accumulated in the subsurface region of ND crystallites. In our experiment it is difficult to follow the rate of migration of nitrogen defects in ND. However, the results of this work have shown that the shape of the N1s photoemission spectra of ND remain unchanged following annealing at different temperatures up to 1420 K, and since the first signs of graphitization are already observed at 1000 K [see C1s photoemission spectrum on Fig. 3(c)], we can conclude that the rate of nitrogen-containing defect diffusion is far lower than the rate of ND graphitization.

The mechanism of ND graphitization has been reviewed in Ref. 31. Briefly the results of this work can be summarised as follows: ND graphitization under annealing begins from the surface towards the crystal bulk and results in the initial formation of bucky diamonds and then eventually in onion-like carbon. The transformation rate of the diamond planes to graphitelike sheets is higher for diamond (111) faces than other surfaces. At the diamond-graphite interface the formation of two curved graphitic sheets from three diamond (111) planes (“zipper”-like mechanism) was observed.<sup>31,61</sup>

Finally, in this work we can rule out degradation of the crystallites due to possible thermally activated bulk diffusion

of hydrogen atoms. Diffusion of hydrogen in *n*-type diamonds such as those doped by phosphorous or nitrogen (the latter type was used in this work) was found to be nonexistent up to 1273 K.<sup>62,63</sup> The formation of N–H and P–H complexes, a surface barrier for diffusion and low solubility of hydrogen in *n*-type diamonds were proposed to explain the absence of diffusion.<sup>62,63</sup> In our experiments, the temperature of the partially graphitized ND sample during hydrogenation was no greater than 500 K. Therefore, according to the literature data<sup>62,63</sup> the diffusion of hydrogen in our nitrogen-doped ND sample would be highly unlikely to occur at this temperature.

To examine experimentally the possible influence of bulk hydrogen diffusion upon the electronic structure of nanodiamond a second partially graphitized nanodiamond sample was investigated following two cycles of hydrogenation and graphitization (data not shown in this paper but were presented to referees). Analysis of the C1s photoemission spectra of this sample shows that the photoemission spectrum following the first atomic hydrogen treatment, coincides with that of nanodiamond after the second atomic hydrogen treatment and also with the C1s spectrum of the nanodiamond sample presented in this paper. Therefore we can conclude that even if hydrogen diffusion into the bulk diamond did occur in our experiments, it would not influence the electronic structure of ND crystallites.

## V. CONCLUSIONS

Hydrogenated and partially graphitized ND particles have been investigated by photoelectron spectroscopy. N1s spectra of the partially graphitized ND have demonstrated the

presence of the nitrogen-containing species in the nanodiamond lattice. We have shown that treatment by atomic hydrogen can be successfully employed to remove the graphitelike layers from ND particle surfaces. This treatment produces hydrogen terminated diamond nanocrystallites. The photoemission studies have revealed that hydrogenation of ND results in a shift of the *sp*<sup>3</sup> component of the C1s peak by 0.9 eV towards a higher binding energy compared to that for a partially graphitized ND sample. We believe that this shift is caused by downward and upward band bending for the hydrogenated and partially graphitized nitrogen-doped ND samples, respectively. This behavior is opposite to that observed for boron-doped diamond crystals. The onset of the ND graphitization was observed at the annealing temperature of 1000 K. The atomic hydrogen treatment could be employed in the deaggregation of ND particles and for their functionalization with hydrogen-containing surface groups (C–H<sub>x</sub>, *x* is 1 or 2). Hydrogen terminated ND particles should possess hydrophobic properties, in contrast with those covered by oxygen-containing groups. Thus hydrogenation of ND particles could enable the preparation of new composite materials through their incorporation into non-polar and hydrophobic media which could open up unique ND applications in biology and electronics.

## ACKNOWLEDGMENTS

We thank George Miller for the construction of the atomic hydrogen gun and for his valuable technical support during the experiment. The project has received funding from the European Community's Sixth Framework Programme, the Marie Curie Incoming International (MIF1-CT-2005-021528) and CCLRC.

\*Corresponding authors. Email addresses:  
yuriy.butenko@ncl.ac.uk, lidija.siller@ncl.ac.uk

<sup>1</sup>A. M. Staver, N. V. Gubareva, A. I. Lyamkin, and E. A. Petrov, *Combust., Explos. Shock Waves* **20**, 567 (1984).

<sup>2</sup>N. R. Greiner, D. S. Phillips, J. D. Johnson, and F. Volk, *Nature (London)* **333**, 440 (1988).

<sup>3</sup>*Ultrananocrystalline diamond: synthesis, properties, and applications*, edited by O. A. Shenderova, and D. M. Gruen (William Andrew Publishing, New York, 2006).

<sup>4</sup>V. L. Kuznetsov, A. L. Chuvilin, E. M. Moroz, V. N. Kolomii-chuk, S. K. Shaichutdinov, Y. V. Butenko, and I. Y. Malkov, *Carbon* **32**, 873 (1994).

<sup>5</sup>A. Kruger, F. Kataoka, M. Ozawa, T. Fujino, Y. Suzuki, A. E. Aleksenskii, A. Y. Vul, and E. Osawa, *Carbon* **43**, 1722 (2005).

<sup>6</sup>Y. Y. Xu, Z. M. Yu, Y. M. Zhu, and B. C. Wang, *Diamond Relat. Mater.* **14**, 206 (2005).

<sup>7</sup>K. Xu and Q. J. Xue, *Phys. Solid State* **46**, 649 (2004).

<sup>8</sup>E. D. Eidelman, V. I. Siklitsky, L. V. Sharonova, M. A. Yagovkina, A. Y. Vul, M. Takahashi, M. Inakuma, M. Ozawa, and E. Osawa, *Diamond Relat. Mater.* **14**, 1765 (2005).

<sup>9</sup>X. Y. Xu, Y. W. Zhu, B. C. Wang, Z. M. Yu, and S. Z. Xie, *J. Mater. Sci. Technol.* **21**, 109 (2005).

<sup>10</sup>A. Kruger, F. Kataoka, M. Ozawa, T. Fujino, Y. Suzuki, A. E.

Aleksenskii, A. Y. Vul, and E. Osawa, *Carbon* **43**, 1722 (2005).

<sup>11</sup>A. Kruger, Y. J. Liang, G. Jarre, and J. Stegk, *J. Mater. Chem.* **16**, 2322 (2006).

<sup>12</sup>S. J. Yu, M. W. Kang, H. C. Chang, K. M. Chen, and Y. C. Yu, *J. Am. Chem. Soc.* **127**, 17604 (2005).

<sup>13</sup>Y. Liu, Z. N. Gu, J. L. Margrave, and V. N. Khabashesku, *Chem. Mater.* **16**, 3924 (2004).

<sup>14</sup>V. S. Bondar, I. O. Pozdnyakova, and A. P. Puzyr, *Phys. Solid State* **46**, 761 (2004).

<sup>15</sup>S. Koizumi, K. Watanabe, F. Hasegawa, and H. Kanda, *Science* **292**, 1899 (2001).

<sup>16</sup>V. L. Kuznetsov, A. L. Chuvilin, Y. V. Butenko, I. L. Malkov, and V. M. Titov, *Chem. Phys. Lett.* **222**, 343 (1994).

<sup>17</sup>B. B. Pate, *Surf. Sci.* **165**, 83 (1986).

<sup>18</sup>V. S. Smentkowski, H. Jansch, M. A. Henderson, and J. T. Yates, *Surf. Sci.* **330**, 207 (1995).

<sup>19</sup>L. Diederich, O. M. Kuttel, E. Schaller, and L. Schlapbach, *Surf. Sci.* **349**, 176 (1996).

<sup>20</sup>F. Maier, M. Riedel, B. Mantel, J. Ristein, and L. Ley, *Phys. Rev. Lett.* **85**, 3472 (2000).

<sup>21</sup>J. B. Cui, J. Ristein, and L. Ley, *Phys. Rev. Lett.* **81**, 429 (1998).

<sup>22</sup>M. Filippi, L. Calliari, G. Pucella, and G. Verona-Rinati, *Surf. Sci.* **573**, 225 (2004).

- <sup>23</sup>J. I. B. Wilson, J. S. Walton, and G. Beamson, *J. Electron Spectrosc. Relat. Phenom.* **121**, 183 (2001).
- <sup>24</sup>M. Tachiki, Y. Kaibara, Y. Sumikawa, M. Shigeno, T. Banno, K. S. Song, H. Umezawa, and H. Kawarada, *Phys. Status Solidi A* **199**, 39 (2003).
- <sup>25</sup>J. Y. Raty, G. Galli, C. Bostedt, T. W. van Buuren, and L. J. Terminello, *Phys. Rev. Lett.* **90**, 037401 (2003).
- <sup>26</sup>T. M. Willey, C. Bostedt, T. van Buuren, J. E. Dahl, S. G. Liu, R. M. K. Carlson, L. J. Terminello, and T. Moller, *Phys. Rev. Lett.* **95**, 113401 (2005).
- <sup>27</sup>A. V. Okotrub, L. G. Bulusheva, V. L. Kuznetsov, Y. V. Butenko, A. L. Chuvilin, and M. I. Heggie, *J. Phys. Chem. A* **105**, 9781 (2001).
- <sup>28</sup>Y. V. Butenko, V. L. Kuznetsov, A. L. Chuvilin, V. N. Kolomiichuk, S. V. Stankus, R. A. Khairulin, and B. Segall, *J. Appl. Phys.* **88**, 4380 (2000).
- <sup>29</sup>A. I. Liamkin, E. A. Petrov, A. P. Ershov, G. V. Sakovich, A. M. Staver, and V. M. Titov, *Dokl. Akad. Nauk SSSR* **302**, 611 (1988).
- <sup>30</sup>V. L. Kuznetsov, Y. V. Butenko, A. L. Chuvilin, A. I. Romanenko, and A. V. Okotrub, *Chem. Phys. Lett.* **336**, 397 (2001).
- <sup>31</sup>V. L. Kuznetsov and Y. V. Butenko, in *Ultrananocrystalline diamond: synthesis, properties, and applications*, edited by O. A. Shenderova and D. M. Gruen (William Andrew Publishing, New York, 2006), Chap. 13, p. 405.
- <sup>32</sup>S. Doniach and M. Šunjić, *J. Phys. C* **3**, 285 (1970).
- <sup>33</sup>J. Di'az, G. Paolicelli, S. Ferrer, and F. Comin, *Phys. Rev. B* **54**, 8064 (1996).
- <sup>34</sup>D. A. Shirley, *Phys. Rev. B* **5**, 4709 (1972).
- <sup>35</sup>A. Laskarakis, S. Logothetidis, and M. Gioti, *Phys. Rev. B* **64**, 125419 (2001).
- <sup>36</sup>R. McCann, S. S. Roy, P. Papakonstantinou, M. F. Bain, H. S. Gamble, and J. A. McLaughlin, *Thin Solid Films* **482**, 34 (2005).
- <sup>37</sup>Y. V. Butenko, S. Krishnamurthy, A. K. Chakraborty, V. L. Kuznetsov, V. R. Dhanak, M. R. C. Hunt, and L. Šiller, *Phys. Rev. B* **71**, 075420 (2005).
- <sup>38</sup>C. Ronning, H. Feldermann, R. Merk, H. Hofsass, P. Reinke, and J. U. Thiele, *Phys. Rev. B* **58**, 2207 (1998).
- <sup>39</sup>C. Kanai, K. Watanabe, and Y. Takakuwa, *Phys. Rev. B* **63**, 235311 (2001).
- <sup>40</sup>A. Bianconi, S. B. M. Hagstrom, and R. Z. Bachrach, *Phys. Rev. B* **16**, 5543 (1977).
- <sup>41</sup>M. Montalti, S. Krishnamurthy, Y. Chao, Y. V. Butenko, V. L. Kuznetsov, V. R. Dhanak, M. R. C. Hunt, and L. Šiller, *Phys. Rev. B* **67**, 113401 (2003).
- <sup>42</sup>G. Francz and P. Oelhafen, *Diamond Relat. Mater.* **4**, 539 (1995).
- <sup>43</sup>J. Robertson and E. P. O'Reilly, *Phys. Rev. B* **35**, 2946 (1987).
- <sup>44</sup>T. Jiang and K. Xu, *Carbon* **33**, 1663 (1995).
- <sup>45</sup>I. Gouzman, R. Brenner, and A. Hoffman, *Surf. Sci.* **333**, 283 (1995).
- <sup>46</sup>I. Kusunoki, M. Sakai, Y. Igari, S. Ishidzuka, T. Takami, T. Takaoka, M. Nishitani-Gamo, and T. Ando, *Diamond Relat. Mater.* **9**, 698 (2000).
- <sup>47</sup>H. Tillborg, A. Nilsson A, B. Hernnas, N. Martensson, and R. E. Palmer, *Surf. Sci.* **295**, 1 (1993).
- <sup>48</sup>R. Kalish, *Diamond Relat. Mater.* **10**, 1749 (2001).
- <sup>49</sup>Y. Dai, D. Dai, C. Yan, B. Huang, and S. Han, *Phys. Rev. B* **71**, 075421 (2005).
- <sup>50</sup>L. Diederich, O. M. Kuttel, P. Ruffieux, T. Pillo, P. Aebi, and L. Schlapbach, *Surf. Sci.* **417**, 41 (1998).
- <sup>51</sup>S. Bhattacharyya, O. Auciello, J. Birrell, J. A. Carlisle, L. A. Curtiss, A. N. Goyette, D. M. Gruen, A. R. Krauss, J. Schlueter, A. Sumant, and P. Zapol, *Appl. Phys. Lett.* **79**, 1441 (2001).
- <sup>52</sup>D. M. Gruen, in *Ultrananocrystalline diamond: synthesis, properties, and applications*, edited by O. A. Shenderova and D. M. Gruen (William Andrew Publishing, New York, 2006), Chap. 5, p. 157.
- <sup>53</sup>P. Zapol, in *Ultrananocrystalline diamond: synthesis, properties, and applications*, edited by O. A. Shenderova and D. M. Gruen (William Andrew Publishing, New York, 2006), Chap. 8, p. 273.
- <sup>54</sup>J. Y. Raty and G. Galli, *Nat. Mater.* **2**, 792 (2003).
- <sup>55</sup>A. S. Barnard, Stability of Nanodiamonds, in *Ultra Nanocrystalline Diamond, Synthesis, Properties and Applications*, edited by O. A. Shenderova and D. M. Gruen (William Andrew Publishing, New York, 2006), Chap. 4, p. 117.
- <sup>56</sup>A. S. Barnard, *Diamond Relat. Mater.* **15**, 285 (2006).
- <sup>57</sup>H. O. Pierson in *Handbook of Carbon, Graphite, Diamond and Fullerenes—Properties, Processing and Applications* (William Andrew Publishing, Noyes, 1993), Chap. 14, p. 337.
- <sup>58</sup>K. Masek, S. Fabik, A. Maskova, N. Tsud, K. Veltruska, K. C. Prince, V. Chab, J. Vyskocil, and V. Matolin, *Appl. Spectrosc.* **60**, 936 (2006).
- <sup>59</sup>G. Francz and P. Oelhafen, *Surf. Sci.* **329**, 193 (1995).
- <sup>60</sup>G. Francz, P. Kania, G. Gantner, H. Stupp, and P. Oelhafen, *Phys. Status Solidi A* **154**, 91 (1996).
- <sup>61</sup>V. L. Kuznetsov, I. L. Zilberberg, Yu. V. Butenko, A. L. Chuvilin, and B. Segall, *J. Appl. Phys.* **86**, 863 (1999).
- <sup>62</sup>C. Saguy, C. Cytermann, B. Fizeer, V. Richter, Y. Avigal, N. Moriya, R. Kalish, B. Mathieu, and A. Deneuve, *Diamond Relat. Mater.* **12**, 623 (2003).
- <sup>63</sup>J. Chevallier, F. Jomard, Z. Teukam, S. Koizumi, H. Kanda, Y. Sato, and A. Deneuve, *Diamond Relat. Mater.* **11**, 1566 (2002).